Physics and Chemistry of the Earth xxx (2015) xxx–xxx

Contents lists available at ScienceDirect

Physics and Chemistry of the Earth

journal homepage: www.elsevier.com/locate/pce

Seasonal drought predictability in Portugal using statistical–dynamical techniques

A.F.S. Ribeiro, C.A.L. Pires *

Instituto Dom Luiz (IDL), Faculdade de Ciências, Universidade de Lisboa, 1749-016 Lisboa, Portugal

ARTICLE INFO

Article history:
Received 10 December 2014
Received in revised form 18 March 2015
Accepted 23 April 2015
Available online xxxx

Keywords:
Long-range forecasts
Predictability
Statistical prediction
Drought index SPI
Precipitation forecasting

ABSTRACT

Atmospheric forecasting and predictability are important to promote adaption and mitigation measures in order to minimize drought impacts. This study estimates hybrid (statistical–dynamical) long-range forecasts of the regional drought index SPI (3-months) over homogeneous regions from mainland Portugal, based on forecasts from the UKMO operational forecasting system, with lead-times up to 6 months. ERA-Interim reanalysis data is used for the purpose of building a set of SPI predictors integrating recent past information prior to the forecast launching. Then, the advantage of combining predictors with both dynamical and statistical background in the prediction of drought conditions at different lags is evaluated. A two-step hybridization procedure is performed, in which both forecasted and observed 500 hPa geopotential height fields are subjected to a PCA in order to use forecasted PCs and persistent PCs as predictors. A second hybridization step consists on a statistical/hybrid downscaling to the regional SPI, based on regression techniques, after the pre-selection of the statistically significant predictors. The SPI forecasts and the added value of combining dynamical and statistical methods are evaluated in cross-validation mode, using the R^2 and binary event scores. Results are obtained for the four seasons and it was found that winter is the most predictable season, and that most of the predictive power is on the large-scale fields from past observations. The hybridization improves the downscaling based on the forecasted PCs, since they provide complementary information (though modest) beyond that of persistent PCs. These findings provide clues about the predictability of the SPI, particularly in Portugal, and may contribute to the predictability of crops yields and to some guidance on users (such as farmers) decision making process.

1. Introduction

Drought episodes in the Iberian Peninsula (IP) have become more frequent and severe (Vicente-Serrano et al., 2014; Sousa et al., 2011), causing several consequences on the socioeconomic and ecological sectors, and leading to major impacts on vegetation (Vicente-Serrano et al., 2013; Gouveia et al., 2012, 2009; Vicente-Serrano, 2007). Extreme episodes, such as the recent 2011–2012, 2004–2005 droughts at Iberia (Trigo et al., 2013; García-Herrera et al., 2007) and the heatwave of 2003 in Europe (Trigo et al., 2005) can seriously affect the agricultural and the hydrologic activities, conditioning the crops and, consequently, requiring adaptation and mitigation measures often entailing high costs. A tendency towards a drier Mediterranean during the 21st century (Giorgi and Lionello, 2008) and the strong variability of the precipitation regime in the IP (Esteban-Parra et al., 1998) enhance the occurrence of droughts and promote the need for drought forecast (either seasonal and climatic), in order to prevent the mentioned impacts.

The predictability of the atmospheric seasonal variability (e.g. Brankovic et al., 1994; e.g. Van den Dool, 1994) has many potential applications, in particular those related to risk management due to drought conditions. Predictions on seasonal time-scales rely on the low-frequency variability of the atmosphere, since the major part of the atmospheric variability show variations on long time scales (seasons and years), which can be predictable to some extent. One of the most important of these low-frequency modes in Europe is the North Atlantic Oscillation (NAO), the dominant mode of winter climate variability over the North Atlantic-European (NAE) region (e.g. Hurrel, 1995), which plays the most important role in precipitation variability over Iberia (Trigo et al., 2004; Rodríguez-Puebla et al., 2001; Pires and Perdigão, 2007). Nevertheless, despite the much lower forecast skill over extratropics than in tropical regions (e.g. Rowell, 1998; Zhu et al., 2014) it is not negligible, and large-scale features has long been regarded as more predictable

* Corresponding author.
E-mail address: clpires@fc.ul.pt (C.A.L. Pires).

http://dx.doi.org/10.1016/j.pce.2015.04.003
1474-7065/

than small scales (Van den Dool and Saha, 1990). In a simple way, low-frequency modes can be interpreted as sources of predictability or "windows of opportunity" of potential predictability: the ability to predict well the low-frequency modes, may lead to a good prediction of the regional features, such as droughts.

Long-range forecasts in Europe have been carried out by many operational meteorological centers, such as the European Center for Medium-Range Weather Forecast (ECMWF), the UK Met Office (UKMO) and the Météo-France. Dynamical predictions systems are widely used for long-range forecasts (e.g. Doblas-Reyes et al., 2009; Vitart et al., 2007), as well as statistical approaches (e.g. Folland et al., 2012; Morid et al., 2007). Given the availability of producing forecasts based on both dynamical and statistical systems, the hybrid combination of statistical and dynamical methods emerged as a commonly and useful approach for long-range forecasts in order to take advantage of both approaches using, for instance: probabilistic forecasting based on Gaussian distribution and deterministic forecasting (Déqué and Stroe, 1994), Bayesian joint probability (BJP) (Peng et al., 2014), space–time principal components (ST-PCs) (Vautard et al., 1996; Sarda et al., 1996) – obtained from the Multi-Singular Spectrum Analysis (MSSA) – regression-based models (Kim and Webster, 2010), and Maximum Covariance Analysis (MCA) (Coelho et al., 2006).

A hybrid approach that has been followed relies in a two-step procedure, in which the predictors are first numerically forecasted and then statistically processed, and finally used to empirically estimate the predict and (e.g. Pires, 1996; Sarda et al., 1996). Recently, using the most recent seasonal Integrated Forecast Systems (IFS) from the EMCWF, Vitart (2014) have shown that the skill of the NAO monthly forecasts have been improving, which is particularly interesting given the importance of this index for the precipitation variability over the NAE region. One of the goals of this work is to take advantage of the skill of the dynamical models in forecasting the low-frequency modes (Peng et al., 2014; Kim et al., 2012), using the first leading Principal Components (PCs) of dynamical seasonal forecasts of the geopotential at 500 hPa (first-step of the hybrid procedure), and then perform a statistical downscaling of those predictors to the regional scale, based on regression techniques (second-step of the hybrid procedure). The first-step of the hybrid procedure also includes the PCs of prior (forecasting initialization date) observations of geopotential, gathering a pool of predictors from both dynamical and statistical backgrounds. The influence of each predictor is here assessed, and the added value of hybridizing dynamical and statistical based predictors is evaluated.

Besides the NAO, evidence is found that other main low-frequency modes are linked to the precipitation regime over IP, which is marked by a strong variability enhance the occurrence of droughts (Esteban-Parra et al., 1998), for instance: the Scandinavian Pattern (SCAND) and the East-Atlantic pattern (EA) (e.g. Rodriguez-Puebla et al., 1998); the East-Atlantic/West Russian Pattern (EA/WR) (Vicente-Serrano and López-Moreno, 2006); which suggests possible drought predictive skills of these teleconnection patterns. Another source of predictability is the influence, though weaker, of the El Niño–Southern Oscillation phenomenon (ENSO) on precipitation (e.g. deCastro et al., 2006; Vicente-Serrano, 2005; Pozo-Vázquez et al., 2001; Rodriguez-Puebla et al., 1998).

An important tool when analyzing drought conditions are the drought indices, which allows for the assignment of different degrees of intensity, duration and spatial extent of droughts. Vicente-Serrano (2005) has discussed the influence of El Niño and La Niña events on droughts in the IP using the Standardized Precipitation Index (SPI), developed by McKee et al. (1993), which is based on a probabilistic approach of the precipitation. Another widely employed drought index is the Palmer Drought Severity Index (PDSI), developed by Palmer (1965) which, besides precipitation, is based on the soil water budget. More recently, Vicente-Serrano et al. (2010) has formulated an index that seeks the combined influence of precipitation and evapotranspiration: the Standardized Precipitation Evaporation Index (SPEI).

The present work aims to contribute to the assessment and improvement of the seasonal predictability of the SPI at a time scale of 3-months (predictand) in the mainland Portugal (western Iberia), with lead-times up to 6 months, based on hybridization techniques. Coelho et al. (2006) has developed a single integrated forecast of seasonal of rainfall that gathers prediction information from three dynamical systems and an empirical model. More recently, Coelho and Costa (2010) discusses the challenges of integrating seasonal forecasts to help the end user managing process. Similarly, the present study also intends to contribute to an improved understanding of the relevance of combining dynamical and statistical techniques in the prediction of droughts over the Portuguese territory, in order to provide some guidance on users (such as farmers) decision making process.

In Section 2 the data and the applied methodology is described, focusing on the two-step hybridization procedure, the selection of the best predictors and the formulation of the statistical downscaling. In Section 3 the results of the forecasts (statistical and hybrid) of the drought index are evaluated according to the lead-time, season and region. A discussion and conclusions follow in Section 4.

2. Data and methods description

2.1. Regional drought index

In this study the Standard Precipitation Index (SPI) is computed based on monthly precipitation time series, providing a measure of anomalies in precipitation (McKee et al., 1993). In order to consider homogeneous climate regions for the computation of regional SPI time-series, the recent high-resolution ($0.2^\circ \times 0.2^\circ$) gridded dataset PT02 developed by Belo-Pereira et al. (2011) is considered. This new dataset based on a dense network of observed data over Portugal (several hundred stations) is a rather good representation of the precipitation regime over Portugal, resulting from the interpolation of observations using the ordinary kriging method, after quality control and homogenization steps.

In this study a Principal Component Analysis (PCA) (Hannachi et al., 2007 and references therein) and a subsequent varimax rotation is applied to the PT02 dataset to search for independent climate sub-regions (Fig. 1). The eigenvalues and eigenvectors are computed from the correlation matrix of the monthly precipitation anomalies with respect to annual cycle. The spatial orthogonal patterns (Empirical Orthogonal Functions (EOFs)) given by the eigenvectors, are proportional to the correlation between the monthly precipitation anomalies and the corresponding principal component time series. The first three modes explain much of the variance fraction (83%) of the precipitation anomalies field, which are retained under orthogonal rotation of the standardized PCs. The varimax orthogonal rotation of the three leading standardized PCs gives three independent sub-regions according to the zero loading lines of the second and third rotated EOFs (REOFs) (Figs. 1 and 2). The zero loading lines from the three REOFs (including the first REOF) would give approximately four regions, however the possible north-eastern region (defined by the first REOF) would be rather small than the other regions and therefore we decided to include it into the north-western region.

While the second REOF indicates the south as a distinct sub-region (hereafter Region 3), coinciding with the driest areas in Portugal, the third REOF points out the north-western region (hereafter Region 1) as a separate climate sub-region, comprising the regions with more cumulative precipitation in Portugal. As a

Please cite this article in press as: Ribeiro, A.F.S., Pires, C.A.L. Seasonal drought predictability in Portugal using statistical–dynamical techniques. J. Phys. Chem. Earth (2015), http://dx.doi.org/10.1016/j.pce.2015.04.003

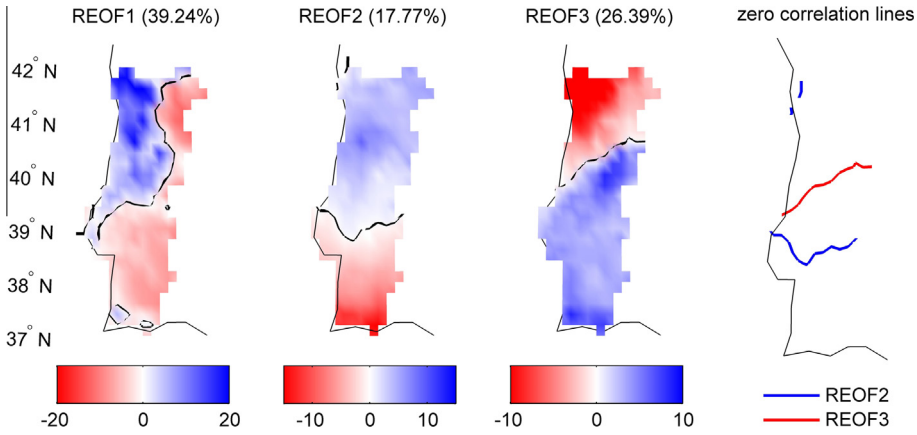

Fig. 1. Varimax REOFs of the monthly precipitation anomalies from the PT02 dataset during 1987–2003. The zero loading lines indicate the regionalization criterion for subsequently regional SPI (3-months) computation. The respective explained variance fraction is indicated in parenthesis.

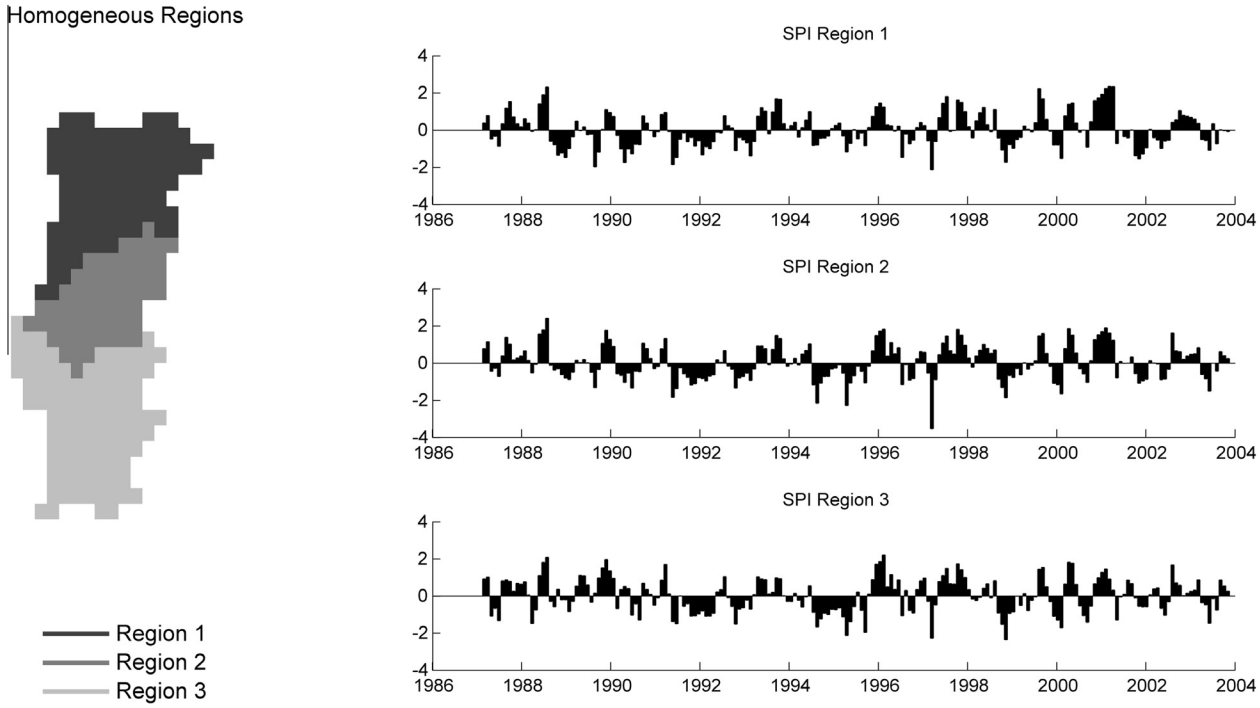

Fig. 2. The three homogeneous regions representation and the respective regional SPI (3-months) computed based on the cumulative precipitation over the north-western (Region 1), the centred (Region 2) and the southern regions (Region 3).

result of the division of these two sub-regions, comes other region on the center (hereafter Region 2) suggesting a different regime of precipitation variability. Recent studies based of the spatial rotated loadings of drought indices (e.g. Raziei et al., 2014; Martins et al., 2012) have also found the north-western and the southern Portugal as dissimilar regions of drought spatial variability.

The regional SPI is computed based on the cumulative precipitation over the three homogenous regions (Fig. 2). One of the advantages of using SPI is that it is a drought index based only on precipitation, and it is more useful than precipitation alone for spatial analysis of droughts, since it compares the precipitation with the average and variance of each location for which the index is calculated. The R Package available at http://sac.csic.es/spei (Vicente-Serrano et al., 2010) is used to compute SPI, which allows for computing SPI at different time scales. For the time scale of 3 months used in this study, the SPI is considered an agricultural drought index, while for longer time scales like 12 months, the SPI should be considered as a hydrological drought index (Vicente-Serrano, 2006). Hereafter, the SPI refers always to the last month of the correspondent time scale (e.g. SPI of December refers to trimester OND)

2.2. Dynamical system data and past observations

In order to build predictors for forecasting the regional SPI, this study uses monthly means of geopotential height at 500 hPa (hereafter referred as z500) from the UKMO forecasting system (ECMWF data arquive), which provides ensemble means (monthly means averaged over all the ensemble members) since 1987 with lead-times up to 6 months, to be used here.

Monthly ERA-Interim reanalysis of the z500 field from the forecasting initialization date is considered for the purpose of build SPI predictors integrating recent past information prior to the forecast launching. For example, a 1 month lead forecast for the SPI of December is initialized on 1 November, whereas 2 month lead forecast for December is initialized on 1 October. For each

Please cite this article in press as: Ribeiro, A.F.S., Pires, C.A.L. Seasonal drought predictability in Portugal using statistical–dynamical techniques. J. Phys. Chem. Earth (2015), http://dx.doi.org/10.1016/j.pce.2015.04.003

December forecast, we use here 6 prior corresponding reanalysis values, covering the forecast lead-times from 1 to 6 months. ERA-Interim reanalysis uses input observations, so reanalysis data is considered as past observations, since it corresponds to what is known before the forecast. The common period 1987–2003 (16 years) between the data from the UKMO forecasting system and the PT02 is used for all data sets considered in this study.

2.3. Two-step hybridization procedure

This study estimates hybrid (statistical–dynamical) predictions of the regional drought index SPI. A key concept of the present methodology is the concept of hybridization, here considered as the combination of predictors of different kinds: the dynamical forecasts and the past observations. A two-step hybridization procedure is adopted: the first-step concerns the application of PCA to the output dynamical forecasting system and also to past observations, in order to build the pool of predictors (PCs) from both dynamical and statistical backgrounds. The second-step regards the statistical downscaling of the predictors, taking the SPI as the predictand, using Multiple Linear Regression (MLR) models. An overview of the main steps of the applied hybridization methodology is resumed in the Fig. 3. The hybridization procedure starts from the forecasts and past observations of the main modes of atmospheric circulation, taking the regional drought index SPI as the variable to predict. Then the significant predictors are selected and the MLR models are established.

2.4. First-step (low-frequency modes computation)

The main modes of atmospheric circulation are computed using PCA of the z500 seasonal (3-months) anomalies over the North Atlantic-European (NAE) region (25°–55°N, 80°W–40°E). The anomalies are computed by removing the seasonal component derived by Seasonal-Trend decomposition based on Loess (STL), a procedure implemented in the R-package *stl*. The STL algorithm enables the seasonal component to change in time (smoothing parameter of 365 days in this case), and is based on locally-weighted regression, or loess (Cleveland et al., 1990), which is a robust method that allows STL to perform rather well even in the cases of extreme observations and/or outliers.

The PCs obtained based on the forecasts of z500 (forecasted PCs hereafter) are obtained by projecting the z500 forecasted field of each lead-time onto the EOFs from the reanalysis data of the respective forecast validation date. We adopt this procedure rather than using EOFs obtained from model runs, necessarily affected by model biases. The forecasted PCs are performed independently for 3-months winter (DJF), 3-months spring (MAM), 3-months summer (JJA) and 3-months autumn (SON). For example, a 1-month lead-time forecast of z500 for 3-months winter is projected onto the EOFs from the reanalysis during the 3-months winter (DJF), and a 2-month lead-time forecast of z500 for 3-months spring are projected onto the EOFs from the reanalysis during the 3-months spring (MAM).

For each lead-time, a benchmark empirical PC is given by the 'persistence', i.e. the observed PCs at the date of initialization of the forecast (persistent PCs hereafter). For example, to the 1-month lead-time forecasted PCs of DJF, it corresponds the persistent PCs based on the reanalysis of NDJ.

Based on the examination of the number of PCs (forecasted and persistent) that explain approximately over 50% of the z500 total variance (explained variance depends on the season and on the lead-time that is considered), the first four persistent PCs and the first four forecasted PCs are retained. Those variance-leading PCs have in general a large-scale and low-frequency signature leading to some potential predictability.

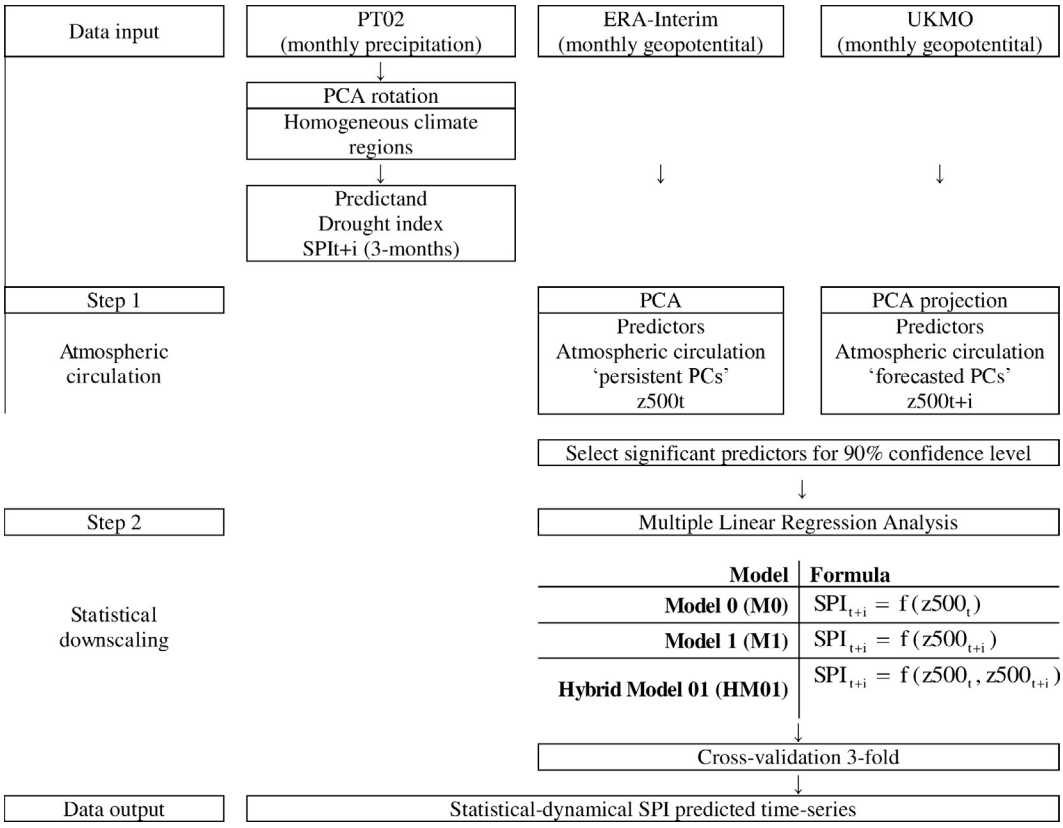

Fig. 3. Schematic view of the applied hybridization technique. The functional dependency of the MLR models are shown in the Step 2, where *i* is the lead-time forecast month and *t* is the forecasting initialization date and *f* Ordinary Linear Regression of arguments.

Please cite this article in press as: Ribeiro, A.F.S., Pires, C.A.L. Seasonal drought predictability in Portugal using statistical–dynamical techniques. J. Phys. Chem. Earth (2015), http://dx.doi.org/10.1016/j.pce.2015.04.003

The first mode of variability based on reanalysis in winter (DJF), spring (MAM), summer (JJA) and autumn (SON) is rather similar to the NAO pattern of circulation. In order to illustrate the persistence predictors, we show in Fig. 4 (right panel) the first four EOFs of z500 anomalies in NDJ (used to compute the winter 1-month lead-time persistence forecasts). There, the first mode projects partly in the negative-phase NAO pattern. The second mode is associated with a high central pressure extending from the American coast up to Europe west coast and also partly projecting on the NAO. This mode has a strong negative correlation with the precipitation in Portugal (see Table 1) (Trigo et al., 2004).The third and fourth modes represent less important modes, associated to longitudinally distributed dipoles over the NAE region.

2.5. Selection of predictors

For each region, lead-time and season, there are eight possible predictors (first four forecasted PCs and first four persistent PCs). Only the statistically significant predictors (for a 90% confidence level) are selected, based on the criterion of the statistical significance of the correlations between the predictors (x) and the predictand (y). The sampling correlations relying on an effective sample size N_{ess} (number of degrees of freedom) have variance given by Eq. (1) and are approximately Gaussian distributed (von Storch and Zwiers, 1999).

$$\mathrm{var}[cor(x,y)_{N_{ess}}] = \frac{1}{N_{ess}-3} \tag{1}$$

In order to compute the N_{ess} of the validation sample to enter in the significance threshold formula of correlation, we suppose that outcomes on different years are independent, hence $N_{ess} = N_{ess}/\mathrm{year} \times Nyears$ where $Nyears = 16$ is the number of years from the study period. For each year and validated season, there are $N_{rea} = 3$ realizations/year corresponding to monthly-delayed SPI (3-months) (e.g. in winter we use SPI (3-months) ending in December, January and February (DJF)) that are partially correlated due to temporal overlapping. For the N_{ess}/year (Eq. (2)) we estimate it for the predictand (y) (Zieba, 2010) through the auto-correlation function at lags of 1 and 2 months as

$$N_{ess}/year = \frac{N_{rea}}{1 + 2\left[\sum_{i=1}^{N_{rea}} (N_{rea} - i) N_{rea}^{-1} \rho_y(i)\right]}, \tag{2}$$

where $\rho_y(1) = 0.90$ and $\rho_y(1) = 0.84$ for the winter SPI, leading to $N_{ess} = 16 * 1.12 \sim 18$. Therefore, by taking two-sided confidence intervals, the minimum value for which the correlation is significant at 90% confidence level, under the null hypothesis of uncorrelated x and y, is 0.41 given by the Eq. (3):

$$C_{90\%} = \frac{q_{95\%}}{\sqrt{N_{ess} - 3}}, \tag{3}$$

where $q_{95\%}$ is the quantile 95% of the standard Gaussian probability density function (pdf). The other seasons give slightly larger *Ness* (due to shorter SPI memory) and smaller $C_{90\%}$ values, thus we keep the conservative threshold 0.41 for the pre-selection of predictors.

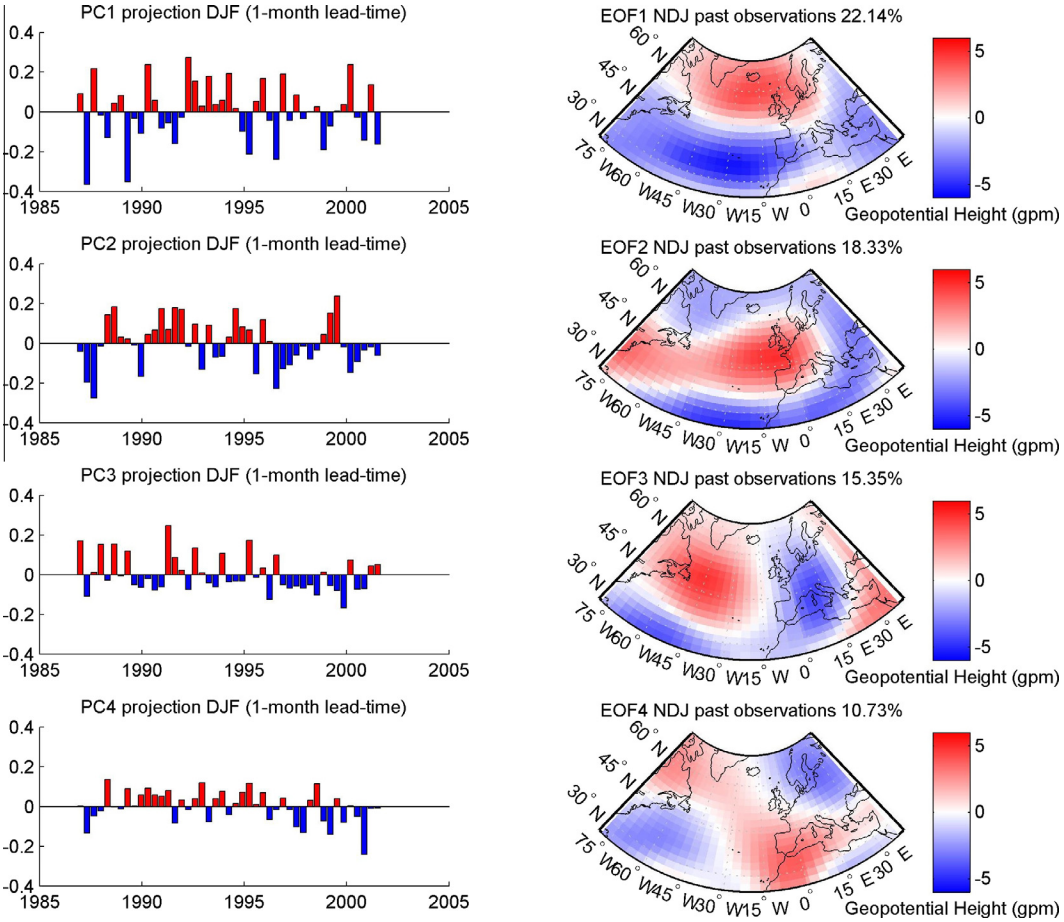

Fig. 4. Illustration of predictors used in 1-month lead-time in winter. Left: First four forecasted PCs based on the UKMO forecasts of 1-month lead-time z500 during the 3-months winter (DJF), i.e. 3 times per year. Right: First four EOFs, based on the past observations from the date of the initialization of the forecasts of 1-month lead-time z500 during the 3-months winter (NDJ).

Please cite this article in press as: Ribeiro, A.F.S., Pires, C.A.L. Seasonal drought predictability in Portugal using statistical–dynamical techniques. J. Phys. Chem. Earth (2015), http://dx.doi.org/10.1016/j.pce.2015.04.003

Table 1
Correlation coefficients between the predictors and the predictands at each homogeneous region (1, 2 and 3), season (DJF, MAM. JJA and SON), and lead-time. PC: Principal Components; PRJ: Principal components projections. For a 90% confidence level, correlations above 0.41 are statically significant (absolute values in bold*).

		Region	PC1	PC2	PC3	PC4	PRJ1	PRJ2	PRJ3	PRJ4			Region	PC1	PC2	PC3	PC4	PRJ1	PRJ2	PRJ3	PRJ4
1-month lead-time	Winter	1	0.08	**−0.79***	−0.03	−0.23	−0.08	**−0.46***	−0.11	−0.08	4-month lead-time	Winter	1	0.06	0.21	−0.34	−0.02	0.09	−0.29	0	−0.32
		2	0.24	**−0.74***	−0.05	−0.26	0.02	**−0.48***	−0.05	−0.04			2	0.08	0.17	−0.38	−0.01	0.14	−0.23	0.08	−0.30
		3	0.35	**−0.62***	−0.08	−0.22	0.10	**−0.45***	0.03	−0.02			3	0.08	0.14	−0.39	−0.04	0.14	−0.25	0.15	−0.29
	Spring	1	0.11	0.25	**−0.62***	0.11	0.10	**−0.52***	0.22	0.14		Spring	1	0.02	−0.30	0.05	−0.03	−0.21	−0.02	−0.14	0.13
		2	0.16	0.28	**−0.57***	−0.03	0.15	**−0.51***	0.12	0.06			2	0.03	−0.18	−0.03	−0.06	−0.14	−0.12	−0.12	0.13
		3	0.16	0.35	**−0.41***	−0.09	0.09	−0.33	0.04	0.17			3	0.1	−0.05	−0.03	−0.14	−0.16	−0.12	−0.17	0.07
	Summer	1	−0.15	−0.05	**−0.41***	0.15	0.01	−0.08	−0.09	0.11		Summer	1	0.15	−0.36	0.17	0.15	−0.05	0.09	−0.09	−0.03
		2	−0.12	−0.05	−0.39	0.17	0.02	−0.05	−0.1	0.06			2	0.16	−0.32	0.13	0.13	0.01	0.06	−0.1	−0.05
		3	−0.24	0.01	−0.34	0.13	0.16	−0.14	−0.05	0.06			3	0.02	−0.27	0.28	0.06	−0.05	0.16	−0.14	−0.06
	Autumn	1	−0.09	−0.11	0.01	0.17	−0.20	−0.12	−0.03	0.25		Autumn	1	−0.06	−0.1	−0.05	−0.11	0.21	0.22	−0.21	−0.08
		2	−0.08	−0.07	0.07	0.32	−0.31	−0.16	0.06	0.2			2	−0.03	−0.1	−0.13	−0.03	0.19	0.24	−0.19	−0.06
		3	−0.02	−0.04	0.11	0.37	−0.3	−0.1	0.16	0.09			3	−0.01	−0.04	−0.11	0.01	0.17	0.23	−0.14	−0.01
2-month lead-time	Winter	1	0.14	**−0.56***	0.06	0.10	0.02	−0.24	−0.08	−0.03			1	**−0.56***	−0.01	−0.04	−0.05	0.04	−0.15	−0.06	−0.37
		2	0.26	**−0.49***	−0.02	0.15	0.12	−0.24	−0.01	−0.01	5-month lead-time	Winter	2	**−0.52***	−0.04	−0.05	−0.12	0.09	−0.08	0	−0.34
		3	0.37	−0.40	−0.07	0.22	0.17	−0.25	0.07	−0.04			3	**−0.51***	0	−0.06	−0.13	0.05	−0.1	0.08	−0.34
	Spring	1	−0.24	−0.13	**−0.46***	−0.14	−0.03	−0.09	0.25	0.14		Spring	1	−0.16	−0.23	0.09	0.14	−0.32	−0.02	−0.07	0.1
		2	−0.26	−0.24	−0.33	−0.15	−0.03	−0.14	0.28	0.16			2	−0.07	−0.17	0.07	0.13	−0.40	−0.16	−0.02	0.14
		3	−0.12	−0.37	−0.19	−0.13	−0.01	−0.17	0.26	0.16			3	0.05	−0.07	0.03	0.14	**−0.42***	−0.15	−0.1	0.22
	Summer	1	−0.01	0.12	**−0.66***	−0.10	0.27	−0.17	−0.02	0.16		Summer	1	0.14	0.2	0.17	0.08	−0.04	−0.11	−0.06	−0.04
		2	0.02	0.19	**−0.63***	−0.08	0.26	−0.13	−0.10	0.10			2	0.20	0.19	0.16	0.01	0	−0.24	0.04	−0.05
		3	0.13	0.33	**−0.60***	−0.13	0.34	−0.26	−0.10	0.02			3	0.14	0.16	0.3	0.02	−0.14	−0.14	0.17	−0.17
	Autumn	1	0.06	−0.04	−0.07	0.11	−0.04	0	−0.08	0.04		Autumn	1	−0.06	−0.2	−0.12	−0.23	0.17	0.09	−0.02	−0.09
		2	0.01	−0.15	−0.05	0.09	−0.02	−0.01	0.05	0.01			2	0.05	−0.16	−0.16	−0.28	0.19	−0.02	0.08	0.01
		3	−0.05	−0.12	−0.03	0.07	−0.06	−0.02	0.09	−0.03			3	0	−0.1	−0.11	−0.14	0.15	−0.06	0.08	0.05
3-month lead-time	Winter	1	0	−0.09	−0.03	0.20	0.01	−0.09	−0.01	−0.15	6-month lead-time	Winter	1	0.38	0.04	−0.16	−0.15	−0.24	−0.24	0.26	−0.28
		2	−0.01	−0.07	−0.06	0.16	0.05	−0.03	−0.02	−0.11			2	**0.42***	0.03	−0.09	−0.2	−0.17	−0.14	0.30	−0.20
		3	−0.04	−0.05	−0.1	0.14	0.08	−0.01	−0.02	−0.11			3	**0.46***	0.04	−0.05	−0.19	−0.17	−0.06	0.32	−0.14
	Spring	1	0.21	−0.14	−0.21	0.12	0.29	0.03	0.08	−0.27		Spring	1	0.13	−0.14	0.18	−0.03	−0.18	0.09	−0.06	−0.02
		2	0.19	−0.1	−0.18	0.04	0.24	0.05	0.08	−0.2			2	0	−0.24	0.04	−0.04	−0.20	0.06	0.05	−0.09
		3	0.08	−0.07	−0.05	−0.04	0.11	0.11	0.03	−0.03			3	−0.16	−0.13	−0.07	0	−0.2	0.08	−0.03	−0.08
	Summer	1	−0.23	0.04	0.15	−0.07	0.21	−0.02	0.27	0.24		Summer	1	−0.03	0.11	−0.02	0.04	0.08	−0.07	0.08	0.12
		2	−0.18	−0.01	0.15	−0.06	0.22	−0.02	0.24	0.19			2	0.05	0.07	0.02	0.13	0.05	−0.09	0.12	0.07
		3	−0.14	0.11	0.07	0.05	0.31	0.08	0.30	0.25			3	0.09	0.08	0.13	0.08	0.17	−0.01	0.07	0.14
	Autumn	1	0.13	−0.15	0.11	−0.03	−0.15	−0.22	−0.15	0.33		Autumn	1	−0.16	−0.13	−0.07	−0.07	0.18	−0.09	0.09	0.06
		2	0.15	−0.19	0.11	0.07	−0.21	−0.2	−0.2	**0.44***			2	−0.11	−0.11	−0.08	0.13	0.19	−0.12	0.15	0.04
		3	0.15	−0.19	0.06	−0.06	−0.20	−0.14	−0.13	0.36			3	0.04	−0.15	−0.08	0.15	0.1	−0.2	0.16	−0.02

The purpose of this approach is to not include noisy or useless predictors in the regression models whose presence would degrade the scores evaluated in validation mode.

2.6. Second-step (statistical downscaling)

For each considered homogeneous region, season and lead-time, a statistical downscaling is performed based on MLR models, during the period 1987–2003, taking each regional SPI time series as predictands. Fig. 3 (on the Step 2) resumes the functional dependency of the MLR models based on ordinary least squares. The *Model 0* (M0) is performed based on the persistent PCs, regarded as a statistical downscaling of the past observations. The next model *Model1* (M1) is based on the UKMO-forecasted PCs denoted as a statistical downscaling of the dynamical forecasts. As a next step, MLR models are established combining predictors from both statistical and dynamical backgrounds. *Hybrid Model 01* (HM01) combines the predictors from M0 and M1, considered as a hybrid downscaling (statistical–dynamical) based on the PCs forecasts of z500 and the observed PCs of z500 from the forecasting initialization date.

2.7. Lead-times of forecast

In this work statistical–dynamical forecasts of droughts are defined as forecasts of the regional drought index SPI. The forecasts of SPI are performed for the 3-months winter (DJF), 3-months spring (MAM), 3-months summer (JJA) and 3-months autumn (SON). Fig. 5 shows a scheme of the forecasting times regarding the winter season, as an example (the same is true for spring, summer and autumn). The lead-time of forecast is defined as the time interval between the dynamical forecast initialization date (cross) and the forecast validation date (black letter) (see lower panel of Fig. 5). The forecast validation dates after a month from the forecast initialization are designated as 1-month lead, and so forth up to 6-month lead.

The monthly view of Fig. 5 shows that each month of the predictand is computed with the same lead-time, for example: the 1-month lead-time winter consists of a December predicted from November, a January predicted from December, and a February predicted from January. This definition was adopted to simplify the integration of data from the past: looking at the seasonal view considering the 1-month lead-time, to each DJF forecast validation period there is a corresponding one month delay NDJ forecast initialization period (dates of the predictors based on observations). The most conventional definition assumes that the 1-month lead-time winter consists of a December predicted from November, a January predicted from November, and a February predicted from November.

Fig. 5 also illustrates the time-scale of 3-months of the SPI, i.e. the SPI memory (white), and the past observations contents (dark gray shadow). In effect, considering the SPI memory of 3-months, the 1-month and 2-month lead-times entail an 'overlap' of information when taking into account the observations of the past on

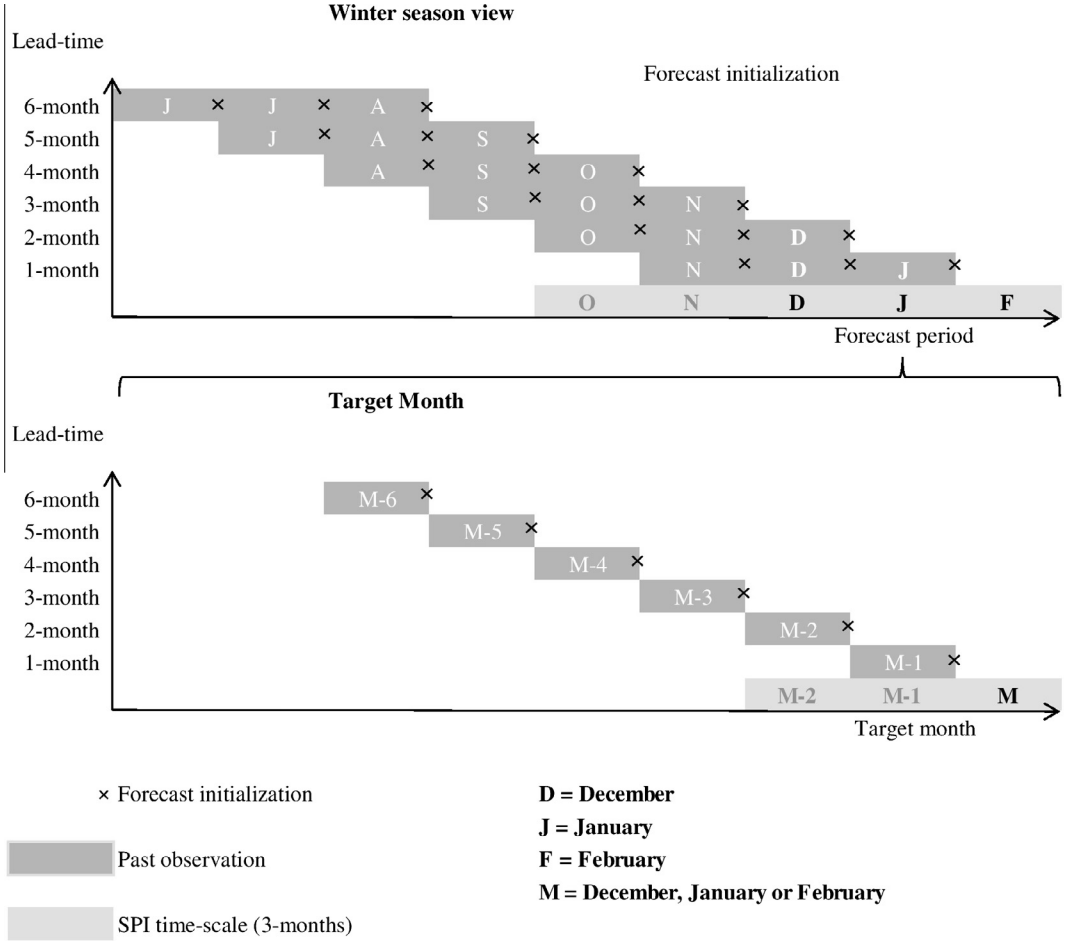

Fig. 5. Scheme of the forecasting lead-times for the winter months as an example (the same is true for the spring and autumn). The dynamical forecast initialization date is denoted as a red cross, and the forecast validation months (effective time of forecasting) are denoted in black letters. The memory of the drought index SPI is represented as a light gray shadow and the past observations contents as a dark gray shadow. In the top is illustrated a scheme of the lead-times during the winter period, and in the bottom is illustrated the same lead-times of each target month contained in the forecast period.

Please cite this article in press as: Ribeiro, A.F.S., Pires, C.A.L. Seasonal drought predictability in Portugal using statistical–dynamical techniques. J. Phys. Chem. Earth (2015), http://dx.doi.org/10.1016/j.pce.2015.04.003

the monthly view. Looking at the seasonal view (from the point of view of score evaluation), the memory of a DJF SPI dates back to October (memory of December), which implies that there is an 'overlap' until the 5-month lead-time on the MLR models. This 'overlap' should improve the forecasting skill at the shorter lead-times, if it had been used all observed precipitation prior to the forecasting initialization time (corresponding to the time-scale of the SPI) as additional predictors (persistent precipitation). In this study, the large-scale predictors with knowledge from the past only refer to the date of initialization of the dynamical forecasts.

2.8. Forecast evaluation

The forecasts and the added value of combining dynamical and statistical methods are evaluated in cross-validation mode, in order to obtain unbiased forecasting scores by removing eventual over-fitting associated to the MLR models, occurring when the same data is used for the fit and for the performance assessment. The basic idea of the cross-validation techniques is to discard part of the data for the MLR model fit, and test the models performance on the data not considered on the fit. In this study the *k*-fold cross-validation (Wilks, 2006) is used, dividing the data into k subsets ($k = 3$), forming a partition of the total available period. In each validation, $k-1$ subsets are used to the fit (the training set), and the leaved out subset is used for prediction (the validation set), ensuring that every subset is used for training and is validated independently.

The forecasting skill is assessed in terms of cross-validated coefficient of determination (R^2), assessing how well a MLR model performs based on information not considered on the model fit. The models performance regarding the occurrence of droughts (SPI < 0) is assessed in terms of contingency tables and associated standard scores: Proportion Correct (PCo), False Alarm Ratio (FAR) and Hit Ratio (HR) (Wilks, 2006). The fraction of forecast occasions that correctly anticipate an event (drought, SPI < 0) or not an event (rainfall, SPI > 0) equally is assessed by the PC score. The hit rate (HR) regards only the correct forecasts of the event of interest (drought), while the ratio of false alarm (FAR) evaluates the number of wrong forecasts of droughts.

3. Results

3.1. Statistical significant predictors

The assessment of the statistical significant predictors is presented in Table 1. Generally, winter in extratropics is the season with the largest potential predictability (e.g. Rowell, 1998; Davies et al., 1997) and displays noteworthy correlation values between predictors and predictands according to Table 1.

Relatively to the persistent PCs during winter, the second mode displays statistically significant correlations at 1, 2, 5 and 6-month lead-times, ranging from 0.79 (1-month lead-time) to 0.42 (6-month lead-time). The results suggest that during winter higher predictive power occur at 1-month lead-time and decrease until 3 and 4-month lead-times, recovering predictability at the 5-month lead-time.

During spring and summer, the third persistent PC also displays statistically significant correlations at 1 and 2-month lead-time. In particular at 2-month lead-time, Table 1 suggests more predictability during summer rather than in winter. On the other hand, during autumn there are not significant correlations using the low-frequency modes based on past observations (persistent PCs). Generally, the north-western region (Region 1), more correlated with the NAO index, records the highest correlation values in all seasons at each lead-time, except for the 6-month lead-time.

In respect to the low-frequency modes based on dynamical forecasts (M1), the winter (Regions 1, 2 and 3) and spring (Regions 1 and 2) display the highest correlation values using the second mode, only at 1-month lead-time. According to the criterion for the selection of significant predictors adopted here, the 5-month lead-time spring forecasts (Regions 3) also displays significant correlation coefficients. The single case in which the autumn season meets the test of significance is the 3-month lead-time forecasts based on the fourth forecasted PC (Region 2).

3.2. Forecasting skill scores

The overall performance of the cross-validation of the MLR models (Step 2) is shown in Table 2 in terms of coefficient of determination (R^2), for the four seasons, the six lead-times and the three homogeneous regions over the Portugal territory. After the criterion of selection of the predictors, the statistical model with the most number of candidate cases is the M0 based on the persistent PCs, followed by M01 and HM01. Winter is the season that is mostly represented in Table 2, suggesting a greater potential for predictability. Hybrid (statistical–dynamical) downscaling (HM01) is evaluated during winter (regions 1, 2 and 3) and spring (regions 1 and 2) at 1-month lead-time (Table 2). Generally, the cross-validated R^2 indicates a good performance of the hybrid model HM01 and the statistical model M0. The predictive performance deteriorates substantially using the model M01 based on the forecasted PCs.

Table 2 shows that the winter (1-month lead-time) is the most predictable season, reaching 52.21% of explained variance by the M01 (region 1), indicating the influence of the second mode of the atmospheric circulation during the previous NDJ. A slight improvement is found at regions 2 and 3 during winter by the HM01 over the M0, similarly to regions 1 and 2 during spring. The downscaling during spring is assessed at 1-month lead-time, reaching 37.7% of explained variance at the region 1. The performance of M0 during spring indicates the influence of the third mode of atmospheric circulation during the previous trimester FMA. Generally the hybridization enhances the seasonal forecasting skill when the performance of each predictor is rather similar and complementary, thus improving the prediction ability when considered together. When the performance of persistence is already rather good separately, hybridization does not improve the forecasting due to the poor performance of forecasted PCs as predictors.

At 2-month lead-time the cross-validated R^2 during winter is reduced to less than half of the explained percentage at 1-month lead-time, and absent at 3 and 4-month lead-time. However, at 5-month lead-time, a recovery in forecast skill is verified, also in accordance to Table 1, indicating the influence of atmospheric circulation during JAS in the winter ahead. The lack of significant scores at 3, 4 and 6-month lead-time during winter is associated to the values of correlation with the predictand very close to the threshold value (Table 1). At the 2-month lead time the summer season displays an over performance rather than in 1-month lead-time. This fact suggests the influence of AMJ predictors in the following summer SPI.

Generally, the predictive performance significantly improves from the south to the north during the winter (except for the 6-month lead-time), spring and summer. The absence of regression models in Table 2 during the autumn season is in agreement to Table 1, similar to the spring and summer seasons for longer lead-times.

Please cite this article in press as: Ribeiro, A.F.S., Pires, C.A.L. Seasonal drought predictability in Portugal using statistical–dynamical techniques. J. Phys. Chem. Earth (2015), http://dx.doi.org/10.1016/j.pce.2015.04.003

Table 2
Percentage skill scores in terms of cross-validated R^2 (%) of 1, 2 and 3-month lead-times, using the possible MLR models for the three regions during the winter, spring, summer and autumn. White cells for a (Season/Region/Lag) display at least one model with positive score, with the best model marked bold*.

		Region	M0	M1	HM01			Region	M0	M1	HM01
1-month lead-time	Winter	1	**52.21***	13.04	51.09	4-month lead-time	Winter	1			
		2	39.87	16.45	**40.12***			2			
		3	15.52	9.11	**16.55***			3			
	Spring	1	34.64	19.92	**37.70***		Spring	1			
		2	25.60	22.01	**31.85***			2			
		3	24.49					3			
	Summer	1	−2.40				Summer	1			
		2						2			
		3						3			
	Autumn	1					Autumn	1			
		2						2			
		3						3			
2-month lead-time	Winter	1	17.70			5-month lead-time	Winter	1	27.57		
		2	11.31					2	23.67		
		3						3	17.22		
	Spring	1	5.68				Spring	1			
		2						2			
		3						3			
	Summer	1	41.14				Summer	1			
		2	36.37					2			
		3	33.75					3		−19.23	
	Autumn	1					Autumn	1			
		2						2			
		1						3			
3-month lead-time	Winter	1				6-month lead-time	Winter	1			
		2						2	3.58		
		3						3	7.44		
	Spring	1					Spring	1			
		2						2			
		3						3			
	Summer	1					Summer	1			
		2						2			
		3						3			
	Autumn	1					Autumn	1			
		2		8.88				2			
		3						3			

Table 3
Winter (1-month lead-time) contingency tables and standard scores for drought identification: PC (Proportion Correct), FAR (False Alarm Ratio) and HR (Hit Ratio).

	Winter										
	1-month lead-time										
		Region 1 Drought observed				Region 2 Drought observed				Region 3 Drought observed	
M0		Yes	No	M0		Yes	No	M0		Yes	No
	Yes	0.38	0.17		Yes	0.42	0.21		Yes	0.44	0.17
	No	0.17	0.38		No	0.10	0.38		No	0.15	0.33
	PC = 0.75	FAR = 0.31	HR = 0.69		PC = 0.79	FAR = 0.33	HR = 0.80		PC = 0.78	FAR = 0.28	HR = 0.75
M01		Yes	No	M01		Yes	No	M01		Yes	No
	Yes	0.27	0.38		Yes	0.35	0.33		Yes	0.35	0.33
	No	0.17	0.38		No	0.13	0.35		No	0.15	0.33
	PC = 0.65	FAR = 0.58	HR = 0.62		PC = 0.71	FAR = 0.48	HR = 0.74		PC = 0.69	FAR = 0.48	HR = 0.71
HM01		Yes	No	HM01		Yes	No	HM01		Yes	No
	Yes	0.38	0.17		Yes	0.46	0.13		Yes	0.41	0.21
	No	0.23	0.31		No	0.13	0.35		No	0.15	0.33
	PC = 0.69	FAR = 0.31	HR = 0.62		PC = 0.81	FAR = 0.21	HR = 0.79		PC = 0.75	FAR = 0.33	HR = 0.74

The winter (1-month lead-time) forecast skill is also evaluated in Table 3 by a 2×2 contingency table and standard scores for drought identification, here considered as SPI values smaller than zero. Here, we restrict the analysis to the above case since it is the only one allowing the comparison of scores among different regions and models. We use the PCo score as a measure of correct forecasts of drought event and nonevent. For a random experiment, PCo is a random variable derived from a binomial pdf with $N_{ess} \sim 18$ (see Section 2.5), hence its average is $E(\mathrm{PCo}) = p = 0.50$ and its standard deviation is

$$\sigma(\mathrm{PCo}) = \sqrt{p(1-p)/N_{ess}} \sim 0.12 \quad (4)$$

The PCo pdf is asymptotically Gaussian, therefore, since the 95% probability interval of a Gaussian pdf is ∼[−2 stds, 2 stds], we get PCo significant at the 95% confidence level if $\mathrm{PCo} \notin [p - 2\sigma(\mathrm{PCo}), p + 2\sigma(\mathrm{PCo})] \sim [0.26, 0.74]$, i.e. the PCo is 95%-statistically

Please cite this article in press as: Ribeiro, A.F.S., Pires, C.A.L. Seasonal drought predictability in Portugal using statistical–dynamical techniques. J. Phys. Chem. Earth (2015), http://dx.doi.org/10.1016/j.pce.2015.04.003

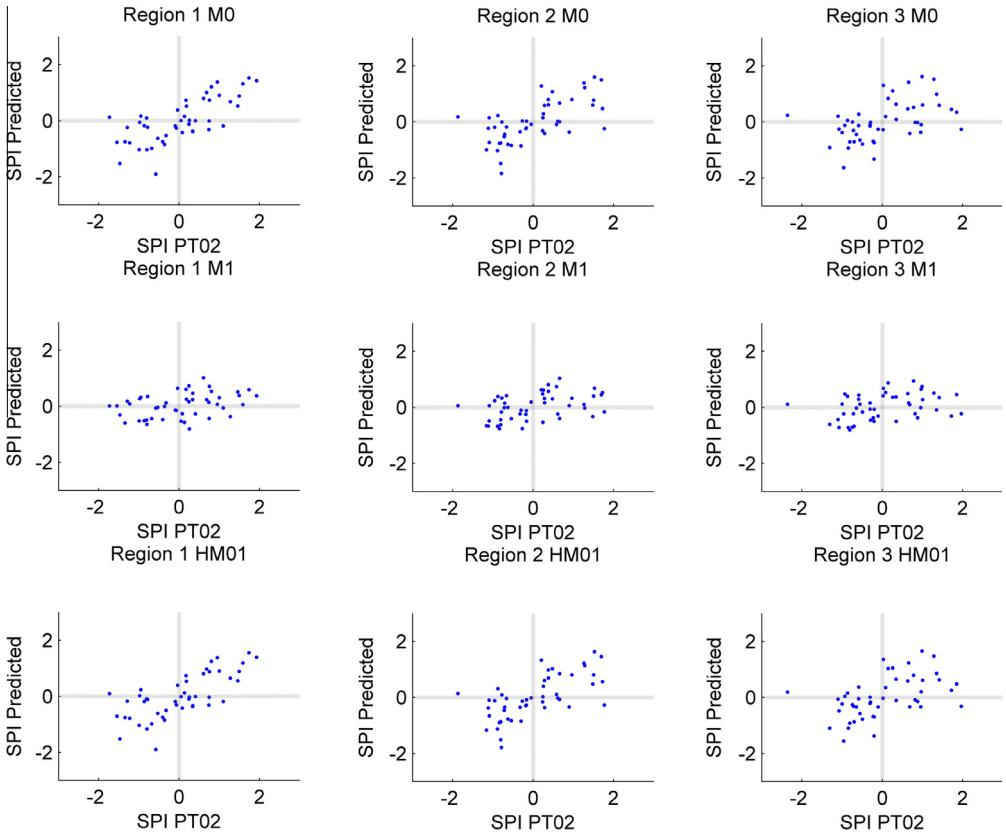

Fig. 6. Winter (1-month lead-time) SPI predicted time-series based on M0 (top row), M1 (center row) and HM01 (bottom row) against observations for the three regions, from left to right.

significant if it is higher than 74%. From Table 3, the PCo of M0, based on persistence reaches the significant values of 75%, 79% and 78% respectively in regions 1, 2 and 3. The hit rate (HR) indicates 69%, 80% 75% of drought events (SPI < 0) correctly forecasted by the M0, in regions 1, 2 and 3 respectively. In region 2, the hybrid model HM01 shows the smaller rate of false alarm (FAR) and the highest PC, whereas all scores are substantially declined by the M1 based on the forecasted PCs.

Scatter plots in Fig. 6 show the forecasted SPI time-series plotted against the observations during winter (1-month lead-time). The second row plots, regarding the M1 illustrate the distribution of the realizations which are highly concentrated around the *xx* axis, indicating a negative bias of the forecasted SPI (and precipitation) variance for the UKMO forecasts. The distributions of scatter points using the M0 (first top row) and the hybrid model HM01 (bottom row) are very similar (due to the small weight given to UKMO outcomes). Furthermore, they have not the biases of the dynamical model but are unable to significantly predict the outlier values of SPI.

4. Discussion and conclusions

In a climate change context, the impacts of droughts in several sectors have become a major concern over the last decades. Drought episodes in the Iberian Peninsula (IP) have become more frequent and the need to predictand prevent drought impacts has been increasing. The regional monthly drought index SPI (3-month) from 1987 to 2003 is considered here as the variable to predict (predictand) over the Portugal territory, where three regions (1-north, 2-central, 3-south) are evaluated during winter, spring, summer and autumn. Each month of the predictand is computed with the same lead-time (see Section 2.3), what may not be as practical for the end user applications, but it provides clues about the predictability of the drought index, and the additional value of the two-step hybridization procedure.

A high resolution precipitation gridded dataset (PT02) was used here, which enables to consider homogeneous climatic by means of a rotated PCA, to guarantee they have not internal precipitation variability. High resolution precipitation data is essential to further improve climate simulations and *e.g.* hydrological applications, given the strong dependency of precipitation on orography and a variety of precipitation regimes in the IP (Belo-Pereira et al., 2011).

An added effort to bring together dynamical seasonal forecasts and statistical methods has come up to address the shortcomings associated to forecasting skills. In order to improve seasonal drought forecasts over Portugal, a two-step hybrid downscaling approach based on statistical–dynamical techniques is presented. This work purposes a two-step hybrid scheme combining dynamical model forecasts and past observations as predictors on a statistical downscaling approach. The performed statistical/hybrid downscaling is based on MLR models, which are widely used, standing out for their modest computing requirements and easy implementation.

The pre-selection of the statistically significant predictors lead to 28 downscaling models with a positive validation score, considering all seasons, lead-times and regions altogether. At the same time, in comparison with the downscaling performed over the training period (without cross-validation, not shown), the explained variance (R^2) of the drought index is smaller, however more accurate, given the overcoming of the problems associated to over-fitting.

A source of predictability over Europe is the influence of the persistent atmospheric circulation patterns. One of the goals of this

Please cite this article in press as: Ribeiro, A.F.S., Pires, C.A.L. Seasonal drought predictability in Portugal using statistical–dynamical techniques. J. Phys. Chem. Earth (2015), http://dx.doi.org/10.1016/j.pce.2015.04.003

study is to take advantage of the skill of the dynamical models in forecasting the low-frequency variability, and enhance the forecasting skill with the additional value of the most recent reanalysis from ECMWF (ERA-Interim) in representing large-scale features. The second (in winter) and third (in spring) persistent PCs of z500 and the second forecasted PC (in both seasons) are the most correlated low-frequency modes of variability at the shorter lead-time (1 month). It would be expected that the first mode of variability exhibited the strongest connection to the drought index because it is commonly linked to NAO, particularly during winter. However, the use of three months and not an average value of the season for the PCA may be capturing the pattern that is more associated with precipitation in other modes.

Results suggest that winter is very predictable, particularly for the shorter lead-time (1-month lead-time). The model M1 rather deteriorates the predictive ability and the hybrid model HM01 exhibit skill scores very similar to that of the M0 (Table 2). However, a very slight improvement is found by the hybrid model HM01 upon the statistical downscaling based on the past M0 (Table 2). The rate of hit a drought event displays the more accurate forecasts using the M0 and the rate of false alarm is substantially discreditable based on the M1 (Table 3). The results propose that the knowledge of the recent past displays the predominant effect, mainly for the shorter lead-time. These findings suggest that the use of the dynamical model forecasts can lead to inaccuracies in the drought index forecasting skill assessment, showing the added value of the integration of past information from reanalysis on the dynamical forecasts.

The persistent PCs which exhibit more influence in winter (DJF) at 1, 2 and 5-month lead-times, are the second mode during NDJ and OND (1 and 2-month lead-times respectively), and the first mode during JAS (5-month lead-time) (see Fig. 5 and Table 2). Part of this influence between DJF and the 1 and 2-month lead-times is related to the here used intrinsic memory of 3-months of SPI predictand, which reflects the influence of the previous atmospheric circulation on agricultural droughts in Portugal. In addition, the results suggests that previous summer and previous early autumn predictors are potential predictors of winter SPI (here 5-month lead-time).

Generally, the predictive performance significantly improves from the region 3 (south) to the region 1 (north) (Table 2), suggesting a dependency in latitude. The region comprising the areas with more cumulative precipitation in Portugal features the best skill scores, reaching more than 50% of explained variance during winter (1-month lead-time) using M0 and HM01 (Table 2).

Taking together the results suggest that both purely statistical downscaling based on the persistent PCs (M0) and hybrid downscaling (HM01) are adequate for estimating the regional SPI (3-months), although the predictive power of the large-scale fields based on past observations (persistence) stands out. The results add substantial information on the use of seasonal predictions for regional drought predictability, in particular in Portugal, and may contribute to the predictability of crops yields.

Conflicts of interest

The authors declare that there are no conflicts of interest.

Acknowledgments

This research was developed at IDL with the support of the Portuguese Foundation for Science and Technology (FCT) through project PTDC/GEOMET/3476/2012 – Predictability assessment and hybridization of seasonal drought forecasts in Western Europe (PHDROUGHT). The authors are thankful to the IPMA (Instituto Português do Mar e da Atmosfera) for the precipitation data used in this study (PT02 precipitation Dataset). The authors are also sincerely thankful to Ricardo Trigo for his valuable suggestions and to two anonymous reviewers for their constructive comments.

References

Belo-Pereira, M., Dutra, E., Viterbo, P., 2011. Evaluation of global precipitation data sets over the Iberian Peninsula. J. Geophys. Res. 116, D20101. http://dx.doi.org/10.1029/2010JD015481.

Brankovic, C., Palmer, T.N., Ferranti, L., 1994. Predictability of seasonal atmospheric variations. J. Clim. 7, 217–237.

Cleveland, R.B., Cleveland, W.S., McRae, J.E., Terpenning, I., 1990. STL: a seasonal-trend decomposition procedure based on loess. J. Official Stat. 6, 3–73.

Coelho, C.A.S., Costa, S.M.S., 2010. Challenges for integrating seasonal climate forecasts in user applications. Curr. Opin. Environ. Sustain. 2, 317–325.

Coelho, C.A.S., Stephenson, D.B., Balmaseda, M., Doblas-Reys, F.J., van Oldenborgh, G.J., 2006. Toward an integrated seasonal forecasting system for South America, America. J. Climate 19, 3704–3721.

Davies, J.R., Rowell, D.P., Folland, C.K., 1997. North Atlantic and European seasonal predictability using an ensemble of multidecadal atmospheric GCM Simulations. Int. J. Climatol. 17, 1263–1284.

deCastro, M., Lorenzo, N., Taboada, J.J., Sarmiento, M., Alvarez, I., Gomez-Gesteira, M., 2006. Influence of teleconnection patterns on precipitation variability and on river flow regimes in the Miño River basin (NW Iberian Peninsula). Climate Res. 32, 63–73.

Déqué, M., Stroe, R., 1994. Formulation of Gaussian probability forecasts based on model extended-range integrations. Tellus 46A, 52–65.

Doblas-Reyes, F.J., Weisheimer, A., Déqué, M., Keenlyside, N., Mcvean, M., Murphy, J.M., Rogel, P., Smith, D., Palmer, T.N., 2009. Addressing model uncertainty in seasonal and annual dynamical ensemble forecasts. Q. J. R. Meteorol. Soc. 135, 1538–1559.

Esteban-Parra, M.J., Rodrigo, F.C., Castro-Díez, Y., 1998. Spatial and temporal patterns of precipitation in Spain for the period 1880–1992. Int. J. Climatol. 18, 1557–1574.

Folland, C.K., Scaife, A.A., Lindesay, J., Stephenson, D.B., 2012. How potentially predictable is the northern European winter climate a season ahead? Int. J. Climatol. 32, 801–808.

García-Herrera, R., Paredes, D., Trigo, R.M., Trigo, I.F., Hernández, E., Barriopedro, D., Mendes, M.A., 2007. The outstanding 2004–05 drought in the Iberian Peninsula: associated atmospheric circulation. J. Hydrometeorol. 8, 469–482.

Giorgi, F., Lionello, P., 2008. Climate change projections for the mediterranean region, global planet. Change 63, 90–104.

Gouveia, C., Trigo, R.M., DaCamara, C.C., 2009. Drought and vegetation stress monitoring in Portugal using satellite data. Nat. Hazards Earth Syst. Sci. 9, 185–195. http://dx.doi.org/10.5194/nhess-9-185-2009.

Gouveia, C.M., Bastos, A., Trigo, R.M., DaCamara, C.C., 2012. Drought impacts on vegetation in the pre- and post-fire events over Iberian Peninsula. Nat. Hazards Earth Syst. Sci. 12, 3123–3137.

Hannachi, A., Jolliffe, I.T., Stephenson, D.B., 2007. Empirical orthogonal functions and related techniques in atmospheric science: a review. Int. J. Climatol. 27, 1119–1152. http://dx.doi.org/10.1002/joc.1499.

Hurrel, J.W., 1995. Decadal trends in the North Atlantic Oscillation: regional temperatures and precipitation. Science 269, 676–679.

Kim, H., Webster, P.J., 2010. Extended-range seasonal hurricane forecasts for the North Atlantic with a hybrid dynamical-statistical model. Geophys. Res. Lett. 37, L21705. http://dx.doi.org/10.1029/2010GL044792.

Kim, H., Webster, P.J., Curry, J.A., 2012. Seasonal prediction skill of ECMWF System 4 and NCEP CFSv2 retrospective forecast for the Northern Hemisphere Winter. Clim. Dyn. 39, 2957–2973.

Martins, D.S., Raziei, T., Paulo, A.A., Pereira, L.S., 2012. Spatial and temporal variability of precipitation and drought in Portugal. Nat. Hazards Earth Syst. Sci. 12, 1493–1501.

McKee, T.B., Doeskin, N.J., Kleist, J., 1993. The relationship of drought frequency and duration to time scales. In: Eighth Conf. on Applied Climatology, American Meteorological Society, pp. 179–184.

Morid, S., Smakhtin, V., Bagherzadeh, K., 2007. Drought forecasting using artificial neural networks and time series of drought indices. Int. J. Climatol. 27, 2103–2111.

Palmer, W.C., 1965. Meteorological Drought. US Weather Bureau, 45, p. 58.

Peng, Z., Wang, Q.J., Bennet, J.C., Schepen, A., Pappenberger, F., Pokhrel P., Wang, Z., 2014. Statistical calibration and bridging of ECMWF System4 for forecasting seasonal precipitation over China. J. Geophys. Res. Atmos., 119, http://dxdoi.org/10.1002/2013JD021162.

Pires, C., 1996. Prévision Atmosphérique à Long-Terme: Un Problème d'Hybridation Statistico-Dynamique. Université Pierre et Marie Curie, Paris, Thèse de Doctorat.

Pires, C.A., Perdigão, R.A.P., 2007. Non-Gaussianity and asymmetry of the winter monthly precipitation estimation from the NAO. Mon. Wea. Rev. 135, 430–448.

Pozo-Vázquez, D., Esteban-Parra, M.J., Rodrigo, F.S., Castro-Díez, Y., 2001. The association between ENSO and winter atmospheric circulation and temperature in the north Atlantic region. J. Clim. 14, 3408–3420.

Raziei, T., Martins, D.S., Bordi, I., Santos, J.F., Portela, M.M., Pereira, L.S., Sutera, A., 2014. SPI modes of drought spatial and temporal variability in portugal:

comparing observations, PT02, and GPCC gridded datasets. Water Resour. Manage., 25634, http://dxdoi.org/10.1007/s11269-014-0690-3.

Rodriguez-Puebla, C., Encinas, A.H., Nieto, S., Garmendia, J., 1998. Spatial and temporal patterns of annual precipitation variability over the Iberian Peninsula. Int. J. Climatol. 18, 299–316.

Rodríguez-Puebla, C., Encinas, A.H., Sáenz, J., 2001. Winter precipitation over the Iberian Peninsula and its relationship to circulation indices. Hydrol. Earth Syst. Sci. 5 (2), 233–244.

Rowell, D.P., 1998. Assessing potential seasonal predictability with an ensemble of multidecadal GCM simulations. J. Clim. 11, 109–119.

Sarda, J., Plaut, G., Pires, C., Vautard, R., 1996. Statistical and dynamical long-range atmospheric forecasts. Exp. Comp. Hybridization Tellus 48A, 518–537.

Sousa, P.M., Trigo, R.M., Aizpurua, P., Nieto, R., Gimeno, L., Garcia-Herrera, R., 2011. Trends and extremes of drought indices throughout the 20th century in the Mediterranean. Nat. Hazards Earth Syst. Sci. 11, 33–51.

Trigo, R.M., Pozo-Vázquez, D., Osborn, T.J., Castro-Díez, Y., Gámiz-Fortis, S., Esteban-Parra, M.J., 2004. North Atlantic Oscillation influence on precipitation, river flow and water re-sources in the Iberian Peninsula. Int. J. Climatol. 24, 925–944.

Trigo, R.M.R., Garcia-Herrera, Díaz, J., Trigo, I.F., Valente, M.A., 2005. How exceptional was the early August 2003 heatwave in France. Geophys. Res. Lett. 32, L10701, http://dx.doi.org/10.1029/2005GL022410.

Trigo, R.M., Añel, J.A., Barriopedro, D., García-Herrera, R., Gimeno, L., Nieto, R., Castillo, R., Allen, M.R., Massey, N., 2013. The record winter drought of 2011–12 in the Iberian Peninsula. Bull. Am. Meteorol. Soc. 94 (9), S41–S45.

Van den Dool, H.M., 1994. Long-range weather forecasts through numerical and empirical methods. Dyn. Atmos. Oceans 20, 247–270.

Van den Dool, H.M., Saha, S., 1990. Frequency dependence in forecast skill. Mon. Weather Rev. 118, 128–137.

Vautard, R., Pires, C., Plaut, G., 1996. Long-range atmospheric predictability using space-time principal components. Mon. Weather Rev. 124, 288–307.

Vicente-Serrano, S.M., 2005. El Niño and LA Niña influence on droughts at different timescales in the Iberian Peninsula. Water Resour. Res. 41, W12415.

Vicente-Serrano, S.M., 2006. Differences in spatial patterns of drought on different time scales: an analysis of the Iberian Peninsula. Water Resour. Manage 20, 37–60. http://dx.doi.org/10.1007/s11269-006-2974-8.

Vicente-Serrano, S.M., 2007. Evaluating the impact of drought using remote sensing in a mediterranean, semi-arid region. Nat. Hazards 40, 173–208. http://dx.doi.org/10.1007/s11069-006-0009-7.

Vicente-Serrano, S.M., López-Moreno, J.I., 2006. The influence of atmospheric circulation at different spatial scales on winter drought variability through a semi-arid climatic gradient in Northeast Spain. Int. J. Climatol. 26 (11), 1427–1453.

Vicente-Serrano, S.M., Beguería, S., López-Moreno, J.I., 2010. A multiscalar drought index sensitive to global warming: the standardized precipitation evapotranspiration index. J. Climate 23, 1696–1718.

Vicente-Serrano, S.M., Gouveia, C., Camarero, J.J., Begería, S., Trigo, R., López-Moreno, J.I., Azorín-Molina, C., Pasho, E., Lorenzo-Lacruz, J., Revuleto, J., Morán-Tejedam E., Sanchez-Lorenzo, A., 2013. Response of vegetation to drought time-scales across global land biomes, PNAS 2013 110 (1) 52–57, http://dx.doi.org/10.1073/pnas.1207068110.

Vicente-Serrano, S.M., Lopez-Moreno, J.I., Berguería, S., Lorenzo-Lacruz, J., Sanchez-Lorenzo, A., García-Ruiz, J.M., Azorin-Molina, C., Morán-Tejeda, E., Revuelto, J., Trigo, R., Coelho, F., Espejo, F., 2014. Evidence of increasing drought severity caused by temperature rise in southern Europe. Environ. Res. Lett. 9, 044001.

Vitart, F., 2014. Evolution of ECMWF sub-seasonal forecast skill scores. Q.J.R. Meteorol. Soc., http://dxdoi.org/10.1002/qj.2256.

Vitart, F., Huddleston, M.R., Déqué, M., Peake, D., Palmer, T.N., Stockdale, T.N., Davey, M.K., Weisheimer, A., 2007. Dynamically-based seasonal forecasts of Atlantic tropical storm activity issued in June by EUROSIP. Geophys. Res. Lett. 34. http://dx.doi.org/10.1029/2007GL030740.

von Storch, H., Zwiers, F.W., 1999. Statistical Analysis in Climate Research. Cambridge University Press, Cambridge, 484.

Wilks, D.S., 2006. Statistical Methods in the Atmospheric Sciences, second ed. Academic Press, Amsterdam.

Zhu, H., Wheeler, M.C., Sobel, A.H., Hudson, D., 2014. Seamless precipitation prediction skill in the tropics and extratropics from a global model. Mon. Weather Rev. 142, 1556–1569.

Zieba, A., 2010. Effective number of observations and unbiased estimators of variance for autocorrelated data – an overview. Metrol. Meas. Syst. 17 (1), 3–16. http://dx.doi.org/10.2478/v10178-010-0001-0.

Please cite this article in press as: Ribeiro, A.F.S., Pires, C.A.L. Seasonal drought predictability in Portugal using statistical–dynamical techniques. J. Phys. Chem. Earth (2015), http://dx.doi.org/10.1016/j.pce.2015.04.003